algorithms

MDPI

Article

Design of a New Energy Microgrid Optimization Scheduling Algorithm Based on Improved Grey Relational Theory

Dong Mo [1], Qiuwen Li [1], Yan Sun [1], Yixin Zhuo [1] and Fangming Deng [2,*]

[1] Power Dispatch and Control Center, Guangxi Power Grid, Nanning 530023, China; mo_d.dd@139.com (D.M.); syhinc094@163.com (Q.L.); gxdwsunyan@126.com (Y.S.); zhuo_yx.dd@gx.csg.cn (Y.Z.)

[2] School of Electrical and Automation Engineering, East China Jiaotong University, Nanchang 330013, China

* Correspondence: 2464@ecjtu.edu.cn

Abstract: In order to solve the problem of the large-scale integration of new energy into power grid output fluctuations, this paper proposes a new energy microgrid optimization scheduling algorithm based on a two-stage robust optimization and improved grey correlation theory. This article simulates the fluctuation of the outputs of wind turbines and distributed photovoltaic power plants by changing their robustness indicators, generates economic operating cost data for microgrids in multiple scenarios, and uses an improved grey correlation theory algorithm to analyze the correlation between new energy and various scheduling costs. Subsequently, a weighted analysis is performed on each correlation degree to obtain the correlation degree between new energy and total scheduling operating costs. The experimental results show that the improved grey correlation theory optimization scheduling algorithm for new energy microgrids proposed obtains weighted correlation degrees of 0.730 and 0.798 for photovoltaic power stations and wind turbines, respectively, which are 3.1% and 4.6% higher than traditional grey correlation theory. In addition, the equipment maintenance costs of this method are 0.413 and 0.527, respectively, which are 25.1% and 5.4% lower compared to the traditional method, respectively, indicating that the method effectively improves the accuracy of quantitative analysis.

Keywords: new energy; microgrid system; robust optimization; grey correlation theory; optimize scheduling algorithm

Academic Editor: Tushar Kanti Roy

Received: 14 November 2024
Revised: 27 December 2024
Accepted: 6 January 2025
Published: 9 January 2025

Citation: Mo, D.; Li, Q.; Sun, Y.; Zhuo, Y.; Deng, F. Design of a New Energy Microgrid Optimization Scheduling Algorithm Based on Improved Grey Relational Theory. *Algorithms* **2025**, *18*, 36. https://doi.org/10.3390/a18010036

1. Introduction

Renewable energy sources such as solar and wind power are characterized by their clean and sustainable nature, making them key tools for reducing carbon emissions and achieving sustainable green development. Traditional energy dispatch methods often rely on fossil fuels, and their strategies typically struggle to balance economic and environmental benefits. These conventional methods are no longer sufficient to meet the requirements for optimizing renewable energy dispatch. Therefore, studying joint optimization dispatch methods for renewable energy under "dual carbon" goals not only helps improve energy utilization efficiency and reduce carbon emissions, but also provides strong support for the sustainable development of the energy industry [1,2].

The uncertainty and volatility of their output cannot be ignored in terms of their impact on microgrid scheduling. Therefore, the impact of new energy on microgrid scheduling is not only reflected in the start stop of thermal power units, but also in the early planning of supporting facilities such as energy storage devices. Therefore, a method is needed to comprehensively quantify the impact of the volatility of new energy outputs on the total

cost of microgrid scheduling and operation, identify key new energy sources that affect microgrid planning, and determine the capacity of wind and photovoltaic units to be invested in order to promote the goal of renewable energy integration [3,4].

Qiu [5] proposes an evaluation system for the capacity of the power grid to accept wind power, but does not quantitatively analyze the various influencing factors; Ye [6] proposes a schedulable potential evaluation algorithm that considers the different needs of dispatchers and users, achieving potential assessments on both the dispatch and user sides of electric vehicles; and Xu [7] constructs an evaluation index system for the static and characteristic indicators of users, achieving a comprehensive quantitative analysis of the regulatory potential of typical users. In view of the above issues, this article defines the indicator of "scheduling potential" to comprehensively represent the degree of correlation between the volatility of new energy outputs and the total cost of scheduling operations. The greater the correlation between a certain new energy and the total operating cost of scheduling, the greater the impact of fluctuations in the output of new energy on the total operating costs, indicating that the scheduling potential of the new energy is greater.

Considering uncertain factors such as the output of new energy in microgrids [8], the existing literature mainly describes the uncertainty of new energy outputs as stochastic optimization [9], robust optimization [10], and distributed robust optimization. At the same time, in order to comprehensively analyze the scheduling potential of new energy, this article needs to construct multiple scenarios to simulate the output of new energy under different levels of fluctuation, which makes the model difficult to solve. To solve the above problems, the literature uses Bender's decomposition algorithm to solve the model [11]. The literature proposes more efficient column and constraint generation algorithms [12]. The Bender's decomposition algorithm belongs to the row constraint generation algorithm, which constructs the main problem using a dual form of sub-problems and has a higher computational complexity compared to the column constraint generation algorithm. Therefore, current decomposition methods tend to favour column and constraint generation algorithms.

The methods for quantitatively analyzing the load that affects power grid planning in the existing algorithm mainly include grey relational analysis [13], wavelet analysis [14], and variable correlation testing. To obtain more intuitive results for a comprehensive analysis index system, it is usually necessary to perform a comprehensive weighted analysis on the various data generated using the analysis [15–17]. The comprehensive weighted analysis algorithms mainly include Analytic Hierarchy Process [18], Entropy Weight Method [19], and the Delphi Method [20]. Among them, the Analytic Hierarchy Process and Delphi Method have strong subjectivity in setting indicator weights, while the Entropy Weight Method analyzes data dispersion and sets indicator weights objectively. In addition to the weighted analysis method by establishing an evaluation index system mentioned above, some of the literature also uses non-weighted analysis methods such as data envelopment analysis [21] and the TOPSIS method [22]. Wang [23] proposed a cost minimization problem to intelligently schedule energy production for microgrids equipped with unstable renewable energy sources and combined heat and power (CHP) generators. Hosseini [24] proposes a novel robust framework for the day-ahead energy scheduling of a residential microgrid comprising interconnected smart users. The above methods have significantly improved results; however, they do not utilize correlation analysis algorithms with weighting, making it difficult to find the optimal solutions for the weakly correlated initial investment cost, environmental management cost, and the total operating cost of the microgrid. The non-weighted analysis method can directly analyze the data methods of the indicator system, but the modelling and calculation are relatively complex and can only achieve qualitative evaluation.

Based on the above analysis, this paper proposes the new energy scheduling potential evaluation method based on grey correlation theory. This method can more accurately analyze the correlation between initial investment costs, environmental governance costs, and the total operating costs of microgrids, thereby effectively reducing the cost of the integrated construction of renewable energy. The specific contributions are as follows:

(1) In order to obtain the economic operation indicators of a microgrid under different levels of fluctuation, this paper establishes a two-stage robust optimization model for the collaborative optimization of renewable energy, energy storage devices, and micro-gas turbine units, with the objective of minimizing the microgrid scheduling and operation costs. The constraints are linearized using the big-M method, and the column and constraint generation algorithm is adopted to solve the model. Additionally, the robustness indicators of wind turbines and distributed photovoltaic power stations are adjusted to simulate the fluctuation of renewable energy output.

(2) In order to identify the key renewable energy sources that influence microgrid planning, this paper proposes an improved grey relational analysis method combined with the entropy weight method to analyze multi-scenario data. This approach determines the correlation between renewable energy sources and various operating costs, as well as the total operating costs of the microgrid. By ranking these correlation values, a quantitative analysis of the impact of renewable energy sources on grid scheduling is achieved.

2. A Two-Stage Robust Optimization Model

2.1. Mathematical Model of Microgrid System

2.1.1. New Energy and Load Uncertainty Model

In the robust optimization model of this article, the uncertain parameters are the output of wind turbines and distributed photovoltaic power plants, as well as the demand for loads. In this article, R represents the range of uncertain parameters as a bounded closed box type uncertain set. At the same time, to effectively improve the conservatism of the robust optimization, this paper introduces robustness indicators, Γ_{wt}, Γ_{pv}, and Γ_{load} measures, to characterize the volatility of uncertain variables [25]. Uncertain set U is represented by Equations (1)–(3):

$$\begin{cases} P_{\mathrm{wt},t} = P^{0}_{\mathrm{wt},t} + r_{\mathrm{wt},t} \cdot \Delta P^{max}_{\mathrm{wt},t} \\ -1 \le r_{\mathrm{wt},t} \le 1 \\ \dfrac{r_{\mathrm{wt},t} \cdot \Delta P^{\max}_{\mathrm{wt},t}}{P_{\mathrm{wt},t}} \le \Gamma_{\mathrm{wt}} \end{cases} \tag{1}$$

$$\begin{cases} P_{\mathrm{pv},t} = P^{0}_{\mathrm{pv},t} + r_{\mathrm{pv},t} \cdot \Delta P^{\max}_{\mathrm{pv},t} \\ -1 \le r_{\mathrm{pv},t} \le 1 \\ \dfrac{r_{\mathrm{pv},t} \cdot \Delta P^{\max}_{\mathrm{pv},t}}{P_{\mathrm{pv},t}} \le \Gamma_{\mathrm{pv}} \end{cases} \tag{2}$$

$$\begin{cases} P_{\mathrm{load},t} = P^{0}_{\mathrm{load},t} + r_{\mathrm{load},t} \cdot \Delta P^{\max}_{\mathrm{load},t} \\ -1 \le r_{\mathrm{load},t} \le 1 \\ \dfrac{r_{\mathrm{load},t} \cdot \Delta P^{\max}_{\mathrm{load},t}}{P_{\mathrm{load},t}} \le \Gamma_{\mathrm{load}} \end{cases} \tag{3}$$

where $P^{0}_{\mathrm{wt},t}$, $P^{0}_{\mathrm{pv},t}$, and $P^{0}_{\mathrm{load},t}$ are the predicted output values and load demand values of wind turbines and distributed photovoltaic power plants during time period t. $P_{\mathrm{wt},t}$, $P_{\mathrm{pv},t}$, and $P_{\mathrm{load},t}$ are the actual output value and the load demand value of the wind turbine and

the distributed photovoltaic power station in the t period. $\Delta P_{\mathrm{wt},t}^{\max}$, $\Delta P_{\mathrm{pv},t}^{\max}$, and $\Delta P_{\mathrm{load},t}^{\max}$ are the maximum fluctuation of the wind turbine, distributed photovoltaic power station, and load in the t period. $r_{\mathrm{wt},t}$, $r_{\mathrm{pv},t}$, and $r_{\mathrm{load},t}$ are the auxiliary variables characterizing the upper and lower limits of the fluctuations of the uncertain variables.

At the same time, to ensure the stable operation of the system, constraints are imposed on the fluctuation range of uncertain variables [26], as shown below:

$$\begin{cases} P_{\mathrm{wt},t}^{0} - \Delta P_{\mathrm{wt},t}^{\max} \le P_{\mathrm{wt},t} \le P_{\mathrm{wt},t}^{0} + \Delta P_{\mathrm{wt},t}^{\max} \\ P_{\mathrm{pv},t}^{0} - \Delta P_{\mathrm{pv},t}^{\max} \le P_{\mathrm{pv},t} \le P_{\mathrm{pv},t}^{0} + \Delta P_{\mathrm{pv},t}^{\max} \\ P_{\mathrm{load},t}^{0} - \Delta P_{\mathrm{load},t}^{\max} \le P_{\mathrm{load},t} \le P_{\mathrm{load},t}^{0} + \Delta P_{\mathrm{load},t}^{\max} \end{cases} \tag{4}$$

2.1.2. Energy Storage Device

The energy storage device in this article selects the battery as the research object and assumes that it is only in a charging or discharging state during operation [27]. The state of charge model of the battery is as follows:

$$\begin{aligned} SOC_t = \quad & SOC_{t-1} + \left[\frac{\chi_{\mathrm{bat},t} \cdot P_{\mathrm{bat},t}^{\mathrm{ch}} \cdot \eta_{\mathrm{ch}}}{E_{\mathrm{EN}}} \right. \\ & \left. - \frac{(1-\chi_{\mathrm{bat},t}) P_{\mathrm{bat},t}^{\mathrm{dis}}}{E_{\mathrm{EN}} \cdot \eta_{\mathrm{dis}}} \right] \Delta t \times 100\% \end{aligned} \tag{5}$$

where SOC_t and SOC_{t-1} represent the state of charge of the battery during time periods t and $(t-1)$, respectively; $P_{\mathrm{bat},t}^{\mathrm{ch}}$ and $P_{\mathrm{bat},t}^{\mathrm{dis}}$ represent the charging and discharging power of the battery during time period t. η_{ch} and η_{dis} are, respectively, the charging and discharging efficiency of energy storage devices. E_{EN} rated battery capacity. $\chi_{\mathrm{bat},t}$ is a 0–1 integer variable, and $\chi_{\mathrm{bat},t}$= 1 represents that the battery is in a charged state during time period t.

The depth of discharge during each charge and discharge cycle of a battery is a key factor affecting its service life. Ignoring this factor will inevitably lead to optimistic optimization results. The relationship between battery discharge depth and equipment life is shown in the Formula (6). Firstly, the cyclic discharge depth is determined by a rainflow counting method, and then its cyclic life can be fitted by power function. However, this formula has a high degree of nonlinearity and is difficult to solve in the model.

$$N_{\mathrm{life}} = N_0 (D_{dod}^{\mathrm{cyc}})^{-k_p} \tag{6}$$

where N_{life} is the number of cycles when the battery reaches its upper limit of life. D_{dod}^{cyc} is the discharge depth of the battery. N_0 is the number of cycles required for the battery to reach its maximum lifespan when operating at 100% discharge depth. The k_p fitting coefficients of the power function are k_p and N_0, and both are the factory parameters of each battery.

To solve the above problems, this article simplifies them into a lifetime model based on the equivalent full cycle number of discharge depth. Firstly, the number of charge and discharge cycles at different discharge depths is converted to the equivalent full cycle number at 100% discharge depth, and it is assumed that the battery undergoes charge and discharge cycles at time t, with a cycle discharge depth equal to the discharge depth of the battery at time $t-1$. The expressions for the equivalent full cycle number and daily equivalent cycle number of a single battery are as follows [28]:

$$D_{\mathrm{dod},t-1} = 1 - SOC_{t-1} \tag{7}$$

$$D_{\mathrm{dod},t}^{\mathrm{cyc}} = D_{\mathrm{dod},t-1} \cdot \chi_{\mathrm{soc},t} \tag{8}$$

$$\chi_{\mathrm{bat},t} = \max\{\chi_{\mathrm{soc},t} - \chi_{\mathrm{soc},t-1}, 0\} \tag{9}$$

$$n_{\mathrm{eq},t} = \left(D^{\mathrm{cyc}}_{\mathrm{dod},t}\right)^{k_P} \tag{10}$$

$$N_{\mathrm{eq}} = \sum_{t=1}^{T} n_{eq,t} \tag{11}$$

where $D_{\mathrm{dod},t-1}$ is the discharge depth during the $t-1$ period. $D^{\mathrm{cyc}}_{dod,t-1}$ is the depth of cyclic discharge for time period t. When $\chi_{\mathrm{SOC},t}$ is a 0–1 integer variable with a value of 1, this indicates the occurrence of a charge discharge cycle during time period t. $\chi_{\mathrm{bat},t}$ is a 0–1 integer variable is used as the number of cycles for the battery. When its value is 1, this indicates that the battery has undergone one charge discharge cycle—that is, the battery has transitioned from a discharged state to a charged state. $n_{\mathrm{eq},t}$ is the equivalent number of full cycles of the battery during time period t, and N_{eq} is the daily equivalent full cycle count of the battery.

2.2. Objective Function

The objective function of the model is to minimize the total cost of the microgrid, which is solved in two stages in this paper. The first-stage objective function is to minimize the initial investment cost in the microgrid, and the second-stage objective function is to minimize the scheduling and operation cost in the microgrid.

$$\min F = C^{\mathrm{inv}} + C_{\mathrm{open}} \tag{12}$$

where C^{inv} represents the total initial investment cost of the microgrid. C_{open} is the operation and maintenance costs of the microgrid equipment.

(1) Initial investment cost.

The initial investment cost in the first-stage objective function is the equipment investment cost for wind turbines, distributed photovoltaic power plants, energy storage devices, and micro-gas turbine units, as follows [29]:

$$\begin{aligned} C^{inv} = \; & E^{\max}_{bat} c_{bat} F_{CRE}(r_{bat}, Y_{bat}) + \\ & \sum_{i=1}^{3} P^{\max}_{i} c_i F_{CRE}(r_i, Y_i) \end{aligned} \tag{13}$$

$$F(r_i, Y_i) = \frac{r_i (1 + r_i)^{Y_i}}{(1 + r_i)^{Y_i} - 1} \tag{14}$$

where $E^{\max}_{\mathrm{bat}}$ is the maximum battery capacity of the energy storage device. $P^{\max}_{i}$ and c_i are the maximum technical output and investment cost per unit power of the i-th type of power equipment, respectively. $F_{\mathrm{CRE}}(r_i, Y_i)$ is the annual capital recovery rate. r_i and Y_i are the discount rate and discount years of the i-th type of power equipment, where the discount years of the energy storage device are the float life.

(2) Operation and maintenance expenses [30].

$$C_{\mathrm{open}} = C^{\mathrm{open}}_{\mathrm{G}} + C_{\mathrm{grid}} + C_{\mathrm{op}} \tag{15}$$

$$C^{\mathrm{open}}_{\mathrm{G}} = \sum_{t=1}^{T} c_{\mathrm{fuel},t} \cdot P_{\mathrm{G},t} + \sum_{t=1}^{T} \sum_{n=1}^{N} k_{n,t} \cdot c_{n,t} \cdot P_{\mathrm{G},t} \tag{16}$$

$$C_{\mathrm{grid}} = \sum_{t=1}^{T} \left(c_{\mathrm{buy},t} P^{\mathrm{buy}}_{\mathrm{M},t} \Delta t - c_{\mathrm{sell},t} P^{\mathrm{sell}}_{\mathrm{M},t} \Delta t\right) \tag{17}$$

$$C_{\text{op}} = \sum_{i=1}^{4} C_{\text{op}}^{i} \cdot P_{i,t} \tag{18}$$

where $C_{\text{G}}^{\text{open}}$, C_{grid}, and C_{op}, respectively, represent the operating costs of the micro-gas turbine, the cost of purchasing and selling electricity for the micro electric vehicle, and the maintenance cost of the equipment. Fuel cost is $c_{\text{fuel},t}$ for time period t. Real-time output of micro-gas turbines is $P_{\text{G},t}$ for time period t. $k_{n,t}$ and $c_{n,t}$ are the emissions of the nth pollutant and the treatment unit price of the micro-gas turbine during time period t. $c_{\text{buy},t}$ and $c_{\text{sell},t}$, respectively, represent the unit price of electricity purchased and sold during time period t. $P_{\text{M},t}^{\text{buy}}$ and $P_{\text{M},t}^{\text{sell}}$ are the power of the microgrid selling electricity to the distribution network during time t. $P_{i,t}$ and C_{op}^{i} are the maintenance cost unit price and output during time period t for energy storage devices, wind turbines, distributed photovoltaic power plants, and micro combustion units, respectively.

2.3. Constraints

2.3.1. Power Balance Constraint [31]

$$P_{wt,t} + P_{pv,t} + P_{\text{bat},t}^{\text{dis}} + P_{\text{M},t}^{\text{buy}} + P_{G,t} = P_{load,t} + P_{\text{M},t}^{\text{sell}} + P_{\text{bat},t}^{\text{ch}} \tag{19}$$

2.3.2. Constraints on Micro Combustion Units

In hourly scheduling, the response speed of micro-gas turbines is relatively fast, so their climbing constraints can be ignored. This article only considers their output constraints, as follows:

$$P_{\text{G}}^{\text{max}} \le P_{\text{G},t} \le P_{\text{G}}^{\text{min}} \tag{20}$$

In the formula, $P_{\text{G}}^{\text{min}}$ is the minimum technical output of the micro-gas turbine.

2.3.3. Constraints on Energy Storage Devices

The energy storage device has constraints on the upper and lower limits of charging and discharging power and the upper and lower limits of the state of charge, and its maximum value is proportional to the maximum capacity of the battery [32]:

$$0 \le P_{\text{bat},t}^{\text{ch}} \le \chi_{\text{bat}} \varepsilon_{\text{ch}} E_{\text{bat}}^{\text{max}} \tag{21}$$

$$0 \le P_{\text{bat},t}^{\text{dis}} \le (1 - \chi_{\text{bat}}) \varepsilon_{\text{dis}} E_{\text{bat}}^{\text{max}} \tag{22}$$

where ε_{ch} and ε_{dis} represent the ratio of the maximum charging and discharging power of energy storage to the maximum capacity of the battery.

State of charge constraint:

$$SOC^{\text{min}} \le SOC_t \le SOC^{\text{max}} \tag{23}$$

$$SOC_{\text{beg}} = SOC_{\text{end}} \tag{24}$$

where SOC^{min} and SOC^{max} are the lower and upper limits of the battery's state of charge, respectively, and to prevent excessive discharge depth from prolonging the battery's life, it is specified that they SOC should not be less than 20%. SOC_{beg} and SOC_{end} are the state of charge of the battery during the scheduling cycle T is the same from beginning to end.

2.3.4. Power Exchange Constraints

$$0 \le P_{\text{M},t}^{\text{buy}} \le \chi_{\text{M},t} \cdot P_{\text{M}}^{\text{buy,max}} \tag{25}$$

$$0 \le P_{\mathrm{M},t}^{\mathrm{sell}} \le (1-\chi_{\mathrm{M},t}) \cdot P_{\mathrm{M}}^{\mathrm{sell,max}} \tag{26}$$

where $P_{\mathrm{M}}^{\mathrm{buy,max}}$ and $P_{\mathrm{M}}^{\mathrm{sell,max}}$, respectively, represent the upper limit of the power sold by microgrids to online distributors. When $\chi_{\mathrm{M},t}$ is a 0–1 integer variable with a value of 1, this indicates that the microgrid purchases electricity from the distribution network during time period t.

3. Comprehensive Evaluation Index System

3.1. Traditional Grey Relational Analysis Theory

(1) Form an analysis matrix [33].

A sequence of indicators consisting of a new energy robustness index $\boldsymbol{Y} = (Y_1, Y_2, \ldots, Y_a)$ and b microgrid scheduling operation costs $\boldsymbol{X} = (X_1, X_2, \ldots, X_b)$. The indicator sequences Y and X together form the analysis matrix.

$$(Y_a, X_1, \cdots, X_b) = \begin{bmatrix} y_a(1) & x_1(1) & \cdots & x_b(1) \\ y_a(2) & x_1(2) & \cdots & x_b(2) \\ \vdots & \vdots & \ddots & \vdots \\ y_a(n) & x_1(n) & \cdots & x_b(n) \end{bmatrix} \tag{27}$$

where n is an integer representing the number of economic cost data sets generated after changing the robustness coefficient.

(2) Generate initial value matrix.

Before conducting correlation analysis, it is necessary to normalize or initialize the data of the analysis matrix to obtain the initial value matrix.

$$\left(Y'_a, X'_1, \cdots, X'_b\right) = \begin{bmatrix} y'_a(1) & x'_1(1) & \cdots & x'_b(1) \\ y'_a(2) & x'_1(2) & \cdots & x'_b(2) \\ \vdots & \vdots & \ddots & \vdots \\ y'_a(n) & x'_1(n) & \cdots & x'_b(n) \end{bmatrix} \tag{28}$$

(3) Generate a difference matrix.

Perform a difference operation on the elements in the initial value matrix according to Formula (29), calculate the difference Δ_{ab} between the robustness index of group a and the economic characteristic index of group b in the nth row, and obtain the difference matrix Δ as follows:

$$\Delta_{ab} = \left| y'_a(n) - x'_b(n) \right| \tag{29}$$

$$\Delta = \begin{bmatrix} \Delta_{a1}(1) & \Delta_{a2}(1) & \cdots & \Delta_{ab}(1) \\ \Delta_{a1}(2) & \Delta_{a2}(2) & \cdots & \Delta_{ab}(2) \\ \vdots & \vdots & \ddots & \vdots \\ \Delta_{a1}(n) & \Delta_{a2}(n) & \cdots & \Delta_{ab}(n) \end{bmatrix} \tag{30}$$

And calculate the maximum $\Delta_{\max}$ and minimum values $\Delta_{\min}$ of the difference matrix using the following formula:

$$\Delta_{\max} = \max(\max\Delta) \tag{31}$$

$$\Delta_{\min} = \min(\min\Delta) \tag{32}$$

(4) Calculation of Grey Correlation Coefficient.

Calculate the correlation coefficient between the robustness index of group a and the economic characteristic index of group b in the nth row $\lambda_{ab}(n)$ and form a correlation coefficient matrix as follows:

$$\lambda_{ab}(n) = \frac{\Delta_{\min} + \rho\Delta_{\max}}{\Delta_{ab}(n) + \rho\Delta_{\max}} \tag{33}$$

In the formula, ρ is a number with a resolution coefficient between 0 and 1, usually taken as 0.5.

By taking the mean of each column in the correlation coefficient matrix, the grey correlation between the robustness index of group a and the economic characteristic index of group b can be obtained, as shown below:

$$r_{ab} = \frac{1}{n}\sum_{i=1}^{n}\lambda_{ab}(i) \tag{34}$$

3.2. Improvement of Resolution Coefficient

The key to grey relational theory is Formula (29), whose calculation results reflect the "closeness" between data. The smaller the calculation result, the stronger the correlation between the data, and the higher the correlation coefficient in Equation (33). The traditional grey relational theory has a resolution coefficient of 0.5 in Equation (33), which results in the "individuality" of the elements being averaged and reduces the accuracy of the model. Therefore, this article maps the idea of triangular fuzzy theory to the dynamic selection of resolution coefficients.

Due to the resolution coefficient being between (0, 1), the two endpoint values are taken as 0.99 and 0.01, as shown below [34]:

$$\rho = \begin{cases} 0.99 & ,\Delta_{ab}(n) = 0 \\ 1 - \dfrac{\Delta_{ab}(n)}{\Delta_{\max}} & ,0 < \Delta_{ab}(n) < \Delta_{\max} \\ 0.01 & ,\Delta_{ab}(n) = \Delta_{\max} \end{cases} \tag{35}$$

3.3. Entropy Weight Method

The entropy weight method can utilize the information reflected by sufficient objective data for weighting. The higher the degree of data dispersion, the greater the weight of this indicator. The characteristics of entropy weight method can highlight the impact of the volatility of new energy output on various scheduling costs of microgrids. Under the same degree of fluctuation, if the operating cost of a certain scheduling is more discrete, it can highlight the impact of new energy on a certain cost and thus evaluate the scheduling potential of new energy on individual costs. The specific solution process is shown in Figure 1.

(1) Matrix preprocessing.

Form an initial matrix of the indicator sequence $X = (X_1, X_2, \ldots, X_b)$ consisting of the operating costs of b microgrids and use the range method for dimensionless processing based on the characteristics of the indicators, where the negative indicators are represented by Equation (36) and the positive indicators are represented by Equation (37).

$$\frac{\delta f}{\delta x} = \frac{[f(t) - f(t-1)]}{[X(t) - X(t-1)]} \tag{36}$$

$$x''_b(n) = \frac{x_b(n) - x_{\min}}{x_{\max} - x_{\min}} \tag{37}$$

where $x_{\max}$ and $x_{\min}$ are the maximum and minimum values of the X_b sequence. Form a matrix with Formulas (36) and (37) and the dimensionless sample, record it as

$X'' = (X''_1, X''_2, \ldots, X''_b)$, and calculate the proportion of the b-th scheduling cost in the total cost using Formula (38).

$$x'''_b(n) = \frac{x''_b(n)}{\sum_{j=1}^{n} x''_b(n)} \tag{38}$$

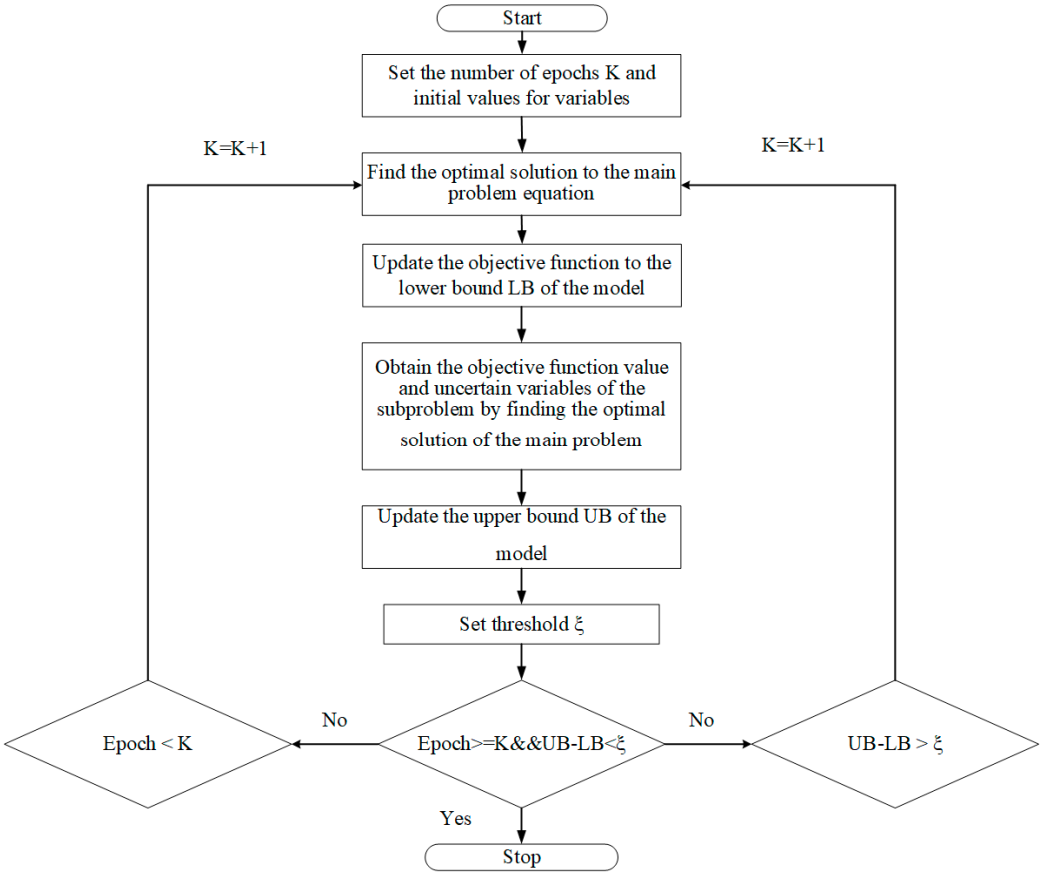

Figure 1. Two-stage robust optimization solution flowchart.

(2) Calculation of entropy value and entropy weight.

The entropy value calculation for indicator b is as follows:

$$T_b = \frac{\sum_{j=1}^{n} x'''_b(n) \cdot \ln x'''_b(n)}{\ln n} \tag{39}$$

The entropy weight calculation for indicator b is as follows:

$$H_b = \frac{1 - T_b}{\sum_{j=1}^{b} (1 - T_b)} \tag{40}$$

Considering the varying degrees of importance of each indicator, this article applies weighted processing to the grey correlation degree calculated by Formula (34). Therefore, the final weighted comprehensive correlation degree is the product of Formulas (34) and (40).

4. Model Solving

4.1. Model Linearization

(1) Equation (9) is determined by the max function, and the equivalent linear form of the number of loop counts is as follows [35]:

$$\chi_{\mathrm{soc},t} - \chi_{\mathrm{soc},t-1} \le \chi_{\mathrm{bat},t} \tag{41}$$

$$\chi_{\mathrm{bat},t} \le \chi_{\mathrm{soc},t} \tag{42}$$

$$\chi_{\mathrm{bat},t} \le 1 - \chi_{\mathrm{soc},t-1} \tag{43}$$

(2) Based on the life model of discharge depth, the Formula (8) defines the discharge depth of the battery at any time and also needs to define the segmentation of the discharge depth at any time, as shown below:

$$D_{\mathrm{dod},t} = \sum_{n=1}^{N} D_{\mathrm{dod},n,t} \tag{44}$$

$$D_{\mathrm{dod},n}^{\min} g_{n,t} \le D_{\mathrm{dod},n} \le D_{\mathrm{dod},n}^{\max} g_{n,t} \tag{45}$$

$$\sum_{m=1}^{M} g_{m,t} = 1 \tag{46}$$

where $D_{\mathrm{dod},n,t}$, $D_{\mathrm{dod},n}^{\min}$, and $D_{\mathrm{dod},n}^{\max}$, respectively, represent the segment, minimum value, and maximum value of the battery discharge depth during time period t. $g_{m,t}$ is a 0–1 integer variable with a value of 1 that represents the state of charge of the battery in the m-th segment during time t.

4.2. Two-Stage Robust Optimization

This article constructs a two-stage robust optimization model and uses column and constraint generation algorithms to solve the optimal economic dispatch scheme under the worst-case scenario. The sub-problems are used to find the worst-case scenario, while the main problem continuously introduces the variables and constraints generated by the sub-problems, thereby narrowing the upper and lower bounds of the objective function to the vicinity of the optimal solution. Describe the original problem in the following form [36]:

$$\begin{cases} \min\limits_{x} \boldsymbol{c}_1^T \boldsymbol{x} + \max\limits_{u} \min\limits_{y\, z} (\boldsymbol{c}_2^T \boldsymbol{y} + \boldsymbol{c}_3^T \boldsymbol{z}) \\ s.t. \quad \boldsymbol{A}\boldsymbol{z} + \boldsymbol{B}\boldsymbol{x} \ge \boldsymbol{d} \\ \quad\quad \boldsymbol{E}\boldsymbol{y} + \boldsymbol{F}\boldsymbol{u} = 0 \\ \quad\quad \boldsymbol{G}\boldsymbol{z} + \boldsymbol{H}\boldsymbol{y} \ge \boldsymbol{h} \\ \quad\quad \boldsymbol{I}\boldsymbol{z} \ge \boldsymbol{k} \\ \quad\quad \boldsymbol{x},\boldsymbol{y},\boldsymbol{u} \ge \boldsymbol{0}, \boldsymbol{z} \in \{0,1\} \end{cases} \tag{47}$$

In the formula, x, y, and z are optimization variables and u is an uncertain variable. The specific variables represented are shown in the Formula (48). A, B, E, F, G, H, I, d, h, and k are constant coefficient matrices corresponding to the constraints [37], where the first constraint represents Equations (21) and (22) in the original problem. The second constraint represents Equation (19) in the original problem. The third constraint represents Equations (20) and (23)–(26) in the original problem. The fourth constraint represents Equations (44)–(46) in the original problem.

$$\begin{cases} x = \left[E_{\text{bat}}^{\max}, P_{\text{WT}}^{\max}, P_{\text{PV}}^{\max}, P_{\text{load}}^{\max}\right]^T \\ y = \left[P_{\text{EOC},t}^{\text{dis}}, P_{\text{EOC},t}^{\text{ch}}, P_{\text{buy},t}, P_{\text{sell},t}, P_{\text{G},t},\right]^T \\ z = \left[\chi_{\text{bat},t}, \chi_{\text{soc},t}, \chi_{\text{M},t}, g_{1,t}, \cdots, g_{m,t}\right]^T \\ u = \left[P_{\text{wt},t}, P_{\text{pv},t}, P_{\text{load},t}\right]^T \end{cases} \tag{48}$$

4.2.1. Main Problem

For each sub-problem in the model that finds the worst-case scenario, new variables are established in the main problem and the main problem is solved. The simplified form of the main problem is as follows:

$$\begin{cases} \min\limits_{x} \boldsymbol{c}_1^T \boldsymbol{x} + \alpha \\ s.t. \quad \alpha \geq \boldsymbol{c}_2^T \boldsymbol{y} + \boldsymbol{c}_3^T \boldsymbol{z} \\ \qquad \boldsymbol{A}\boldsymbol{z}_l + \boldsymbol{B}\boldsymbol{x} \geq \boldsymbol{d} \\ \qquad \boldsymbol{E}\boldsymbol{y}_l + \boldsymbol{F}\boldsymbol{u}_l = 0 \\ \qquad \boldsymbol{G}\boldsymbol{z}_l + \boldsymbol{H}\boldsymbol{y}_l \geq \boldsymbol{h} \\ \qquad \boldsymbol{I}\boldsymbol{z}_l \geq \boldsymbol{k} \\ \qquad \boldsymbol{x},\boldsymbol{y},\boldsymbol{u} \geq \boldsymbol{0}, \boldsymbol{z} \in \{0,1\} \\ \qquad \forall l \in k \end{cases} \tag{49}$$

where α is the auxiliary variable of the sub-problem. k is the total number of iterations of the model. y_l and z_l are the solution to the sub-problem after l iterations. The u_l is to find the worst-case scenario in the uncertain set after one iteration.

4.2.2. Sub-Problems

The sub-problem is used to find the worst-case scenario and return the scenario to the main problem. The simplified form of the sub-problem is as follows:

$$\begin{cases} \max\limits_{u} \min\limits_{y\,z} (c_2^T y + c_3^T z) \\ s.t. \quad \boldsymbol{E}\boldsymbol{y}_l + \boldsymbol{F}\boldsymbol{u}_l = 0 \\ \qquad \boldsymbol{G}\boldsymbol{z}_l + \boldsymbol{H}\boldsymbol{y}_l \geq \boldsymbol{h} \\ \qquad \boldsymbol{I}\boldsymbol{z}_l \geq \boldsymbol{k} \\ \qquad \boldsymbol{y}_l, \boldsymbol{u}_l \geq \boldsymbol{0}, z_l \in \{0,1\} \\ \qquad \forall l \in k \end{cases} \tag{50}$$

Solving the max–min bilayer problem in the above equation, the inner min problem is transformed into the max form according to the dual theory, and it is solved uniformly with the outer max problem [38].

4.3. Solution Process

(1) Set the iteration number $l = 0$, give a set of uncertain variables $\boldsymbol{u}$ as the initial worst-case scenario, and set the upper bound UB $= +\infty$ and lower bound of the collaborative optimization model to $LB = -\infty$.

(2) Solve the main problem Equation (49) based on the worst-case scenario u_1^*, obtain the optimal solution, and update the objective function to the lower bound LB of the model.

(3) Substitute the optimal solution obtained in step (2) into Equation (50) to solve the sub-problem, obtain the objective function value and uncertain variables after solving the sub-problem u_{k+1}^*, and update the upper bound UB of the model.

(4) Set a threshold ξ, and when the k-th iteration is reached, if UB-LB < ξ, stop the model iteration and output the iterated objective function F and the optimal solution u_k^*,

y_k^*, x_k^*. When UB-LB $\geq \xi$, add new variables and constraints, and make $k = k + 1$, and return to step (2) until the result meets the accuracy requirements.

5. Case Studies Analysis

5.1. Data Explanation

This article selects the load curve of a typical 24 h day in spring and optimizes the output curves of wind turbines and photovoltaic power plants. The real-time electricity prices for demand-side loads and power interactions between microgrids and distribution networks in this model are shown in Figure 2.

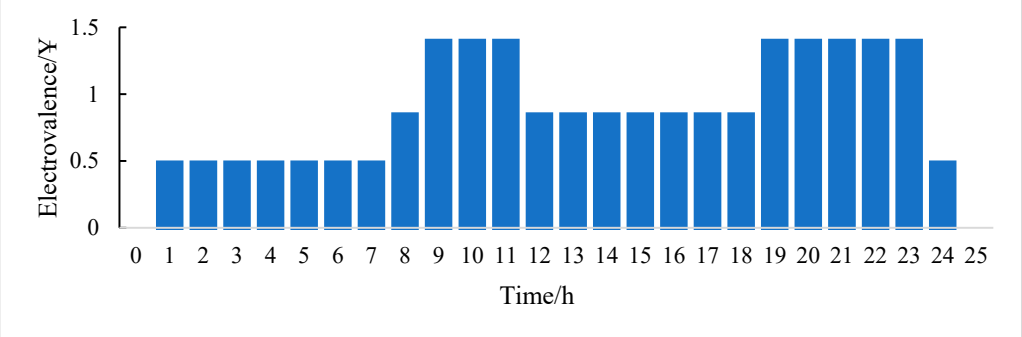

Figure 2. Real-time electricity price of microgrid.

The discount rate r for the micro-gas turbine unit, new energy, and energy storage device in the text is set to 0.08, and the ratio ε_{ch} and ε_{dis} of the maximum charging and discharging power of energy storage to the maximum capacity of the battery is 0.25. The robustness index of load power Γ_{load} is always 0.15, while the robustness indexes Γ_{wt}, Γ_{pv}, and the initial value of the wind turbines and photovoltaic power plants are all 0.05. During the model building process, the operating parameters of each unit are shown in Table 1.

Table 1. Parameters of the microgrid model.

Unit Name	Parameter Name	Value Taking
Micro-gas turbine unit	Unit output upper limit P_G^{max}/kW	500
	Lower limit of unit output P_G^{min}/kW	50
	Fuel cost c_{fuel}/(¥/kWh)	0.6
	Discounted Y_G years/year	15
New energy	Discounted Y_{wt} years/year	20
	Discounted Y_{pv} years/year	15
Energy storage device	Lower limit of state of charge	0.1
	Upper limit of state of charge	0.9
	Initial state of charge	0.5
	Charge and discharge efficiency	0.95
	Discounted Y_{bat} years/year	10
Switching power of distribution network	Power purchase upper limit $P_M^{sell,max}$/kW	400
	Upper limit of electricity sales power $P_M^{buy,max}$/kW	400

In the model presented in this article, the micro-gas turbine unit generates a series of polluting gasses during operation. Due to the fact that wind and solar power generation do not produce polluting gasses, they will not be discussed. The environmental parameters of the microgrid are shown in Table 2.

Table 2. Environmental parameters of miniature gas turbine set.

Pollutant Gasses	Emission Coefficient (g/kWh)	Governance Cost (JPY/kg)
CO_2	889	0.210
SO_2	1.8	1.842
NO_x	4.6	62.964

5.2. Multi Scenario Sample Data Generation

In the model, the fluctuation degree in the wind turbine and photovoltaic power stations is reflected in the value of robustness indexes Γ_{wt} and Γ_{pv}. To accurately assess the impact of the volatility of new energy outputs on grid planning, the initial group sample data are first generated when $\Gamma_{wt} = \Gamma_{pv} = 0.03$. Subsequently, while the robustness index of the wind turbine $\Gamma_{wt} = 0.03$ remains unchanged, the robustness index of the photovoltaic power station is gradually increased from 0.03 to 0.08, and a series of operating cost data affected by photovoltaic output fluctuations is obtained. Finally, while the robustness index of the photovoltaic power station $\Gamma_{pv} = 0.03$ remains unchanged, the robustness index of the wind turbine is gradually increased from 0.03 to 0.08, and a series of operating cost data affected by the output fluctuation of the wind turbine are obtained. The final generated sample data are shown in Table 3.

Table 3. Operating costs under changes in robustness indicators Γ_{wt} and Γ_{pv}.

Γ_{wt}	Γ_{pv}	Initial Investment Cost/JPY	Equipment Maintenance Cost/JPY	Environmental Governance Costs/JPY	Total Cost of Microgrid/ JPY	Time /ms
0.03	0.03	181,472.08	12,967.28	4648.24	203,980.58	32.91
	0.04	181,307.14	19,031.09	4702.38	202,407.29	31.69
	0.05	181,116.65	19,154.91	4749.62	202,650.68	30.47
	0.06	180,994.28	19,276.89	4786.97	202,865.76	29.25
	0.07	180,863.33	19,386.59	4821.71	203,026.18	28.04
	0.08	180,712.29	19,497.45	4856.18	203,264.19	26.90
0.04	0.03	180,572.62	19,543.18	4882.06	203,417.38	25.78
	0.04	180,361.24	19,597.53	4924.20	203,675.53	24.55
	0.05	179,946.72	19,646.31	4971.03	203,892.77	23.32
	0.06	179,815.43	19,700.12	5021.37	204,016.66	22.15
	0.07	179,693.21	19,752.88	5077.69	204,139.46	21.03
	0.08	179,565.17	19,807.91	5124.58	204,259.25	19.98
0.05	0.03	179,447.52	19,866.50	5189.23	204,374.19	18.93
	0.04	179,304.45	19,916.67	5248.69	204,419.32	17.88
	0.05	179,154.07	20,072.35	5300.18	204,526.60	16.82
	0.06	179,033.22	20,251.77	5357.24	204,642.23	15.94
	0.07	178,288.53	21,251.08	5373.06	204,912.67	15.16
	0.08	178,272.26	21,369.44	5392.10	205,033.80	14.37
0.06	0.03	178,149.82	21,472.37	5416.17	205,094.18	13.60
	0.04	178,103.59	21,593.97	5431.05	205,168.57	12.78
	0.05	178,067.16	21,769.91	5447.43	205,239.50	12.14
	0.06	178,003.27	21,856.37	5471.38	205,304.46	11.59
	0.07	177,956.54	22,116.75	5469.32	205,445.63	10.97
	0.08	177,815.17	22,377.18	5467.28	205,586.80	10.56
0.07	0.03	177,673.75	22,637.52	5465.22	205,727.96	10.22
	0.04	177,532.32	22,897.90	5463.17	205,869.13	9.83
	0.05	177,390.89	23,158.29	5461.12	206,010.30	9.42
	0.06	177,265.81	23,317.00	5465.10	206,047.91	8.99
	0.07	177,140.72	23,475.71	5469.08	206,085.52	8.67
	0.08	177,015.64	23,634.43	5473.06	206,123.13	8.34

Table 3. *Cont.*

Γ_{wt}	Γ_{pv}	Initial Investment Cost/JPY	Equipment Maintenance Cost/JPY	Environmental Governance Costs/JPY	Total Cost of Microgrid/ JPY	Time /ms
0.08	0.03	176,890.56	23,793.14	5477.04	206,160.73	8.06
	0.04	176,765.47	23,951.85	5481.02	206,198.34	7.84
	0.05	176,640.39	24,110.56	5485.00	206,235.95	7.51
	0.06	176,533.32	24,261.97	5489.11	206,234.59	7.26
	0.07	176,426.25	24,413.38	5493.23	206,233.23	7.09
	0.08	176,319.18	24,564.79	5497.34	206,231.87	6.81

From Table 3, it can be seen that as Gamma wt and Gamma PV represent the deviation between predicted and actual costs, as Gamma wt and Gamma PV decrease, i.e., as the number of iterations increases, the solving time of the column and constraint generation algorithms gradually increases, and the time increases faster when the values of Gamma wt and Gamma PV are larger.

Due to the excessive number of scenes, only the optimization results of $\Gamma_{wt} = \Gamma_{pv} = 0.05$ (Figure 3), $\Gamma_{wt} = 0.05$, $\Gamma_{pv} = 0.08$ (Figure 4), and $\Gamma_{wt} = 0.08$, $\Gamma_{pv} = 0.05$ (Figure 5) are presented here.

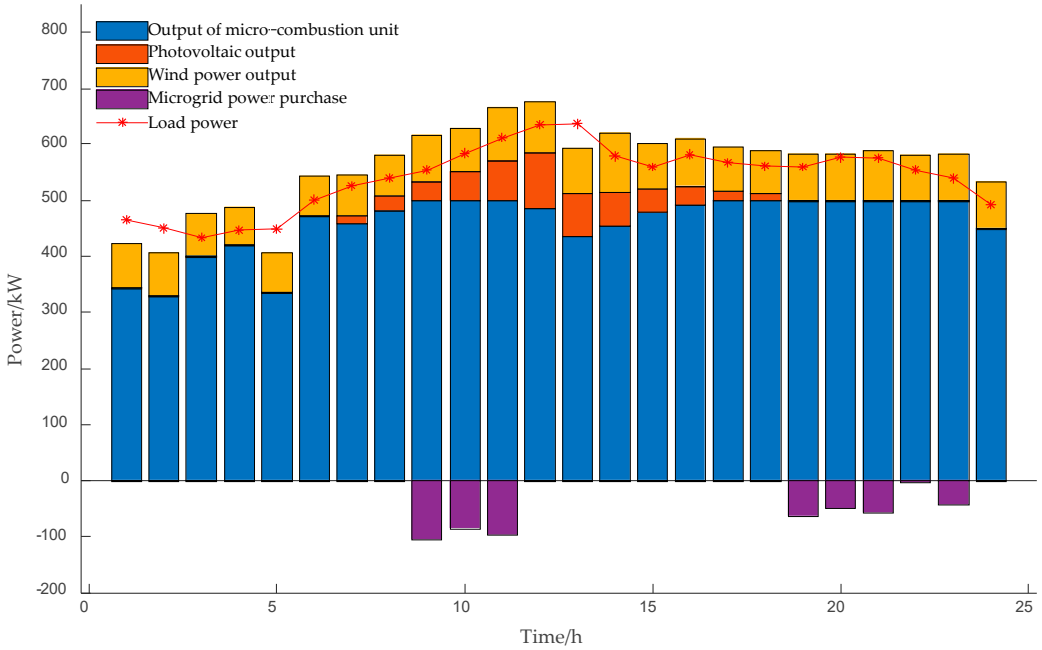

Figure 3. Optimization and dispatch results of microgrid ($\Gamma_{wt} = \Gamma_{pv} = 0.05$).

From the comparison between Figures 3 and 4, it can be seen that the increase in the fluctuation of photovoltaic power station output has a significant impact on the scheduling of typical spring days from 11:00 to 15:00. The output of micro combustion units increases significantly, photovoltaic consumption decreases significantly, and there are no significant fluctuations in electricity sales. From the comparison between Figures 3 and 5, it can be seen that the increase in fluctuation of wind turbine output has a greater impact on typical spring days from 11 a.m. to 15 p.m. and from 20 to 23 p.m. The output of micro combustion units significantly increases during lunchtime, while the wind power output of the system is lower at night. Therefore, power balance is maintained by purchasing electricity.

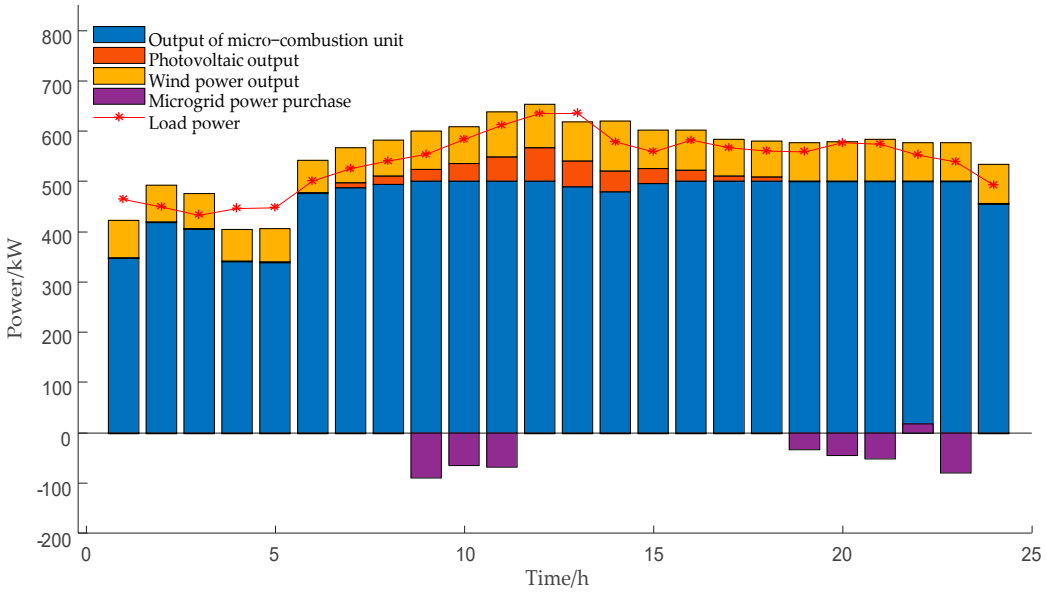

Figure 4. Optimization and dispatch results of microgrid ($\Gamma_{wt} = 0.05, \Gamma_{pv} = 0.08$).

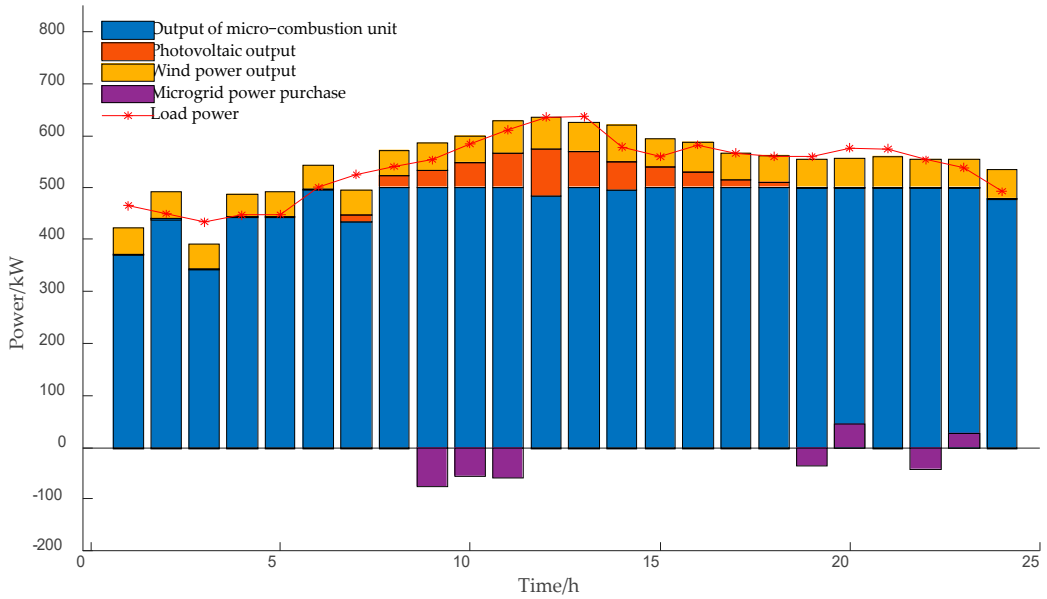

Figure 5. Optimization scheduling results of microgrid ($\Gamma_{wt} = 0.08, \Gamma_{pv} = 0.05$).

In summary, when the fluctuations in wind turbine and photovoltaic power plant outputs increase, the system chooses to maintain power balance by increasing the output of micro combustion units at noon, and the impact and mode of the two are similar. But at night, the fluctuations in wind turbines have a significant impact on the scheduling and operation of microgrids, especially in terms of the amount of electricity purchased by microgrids. This is because the uncertainty of the wind still exists at night, and the factors such as the ambient temperature at night will also affect the performance of the wind turbine, making its output power not as stable as during the day. The photovoltaic power station mainly relies on solar radiation for power generation, and its output power fluctuates with the change in solar radiation intensity, angle, and other factors during the day. At midday, when the solar radiation is relatively stable, the power fluctuations are relatively small. At night, without solar radiation, the output of the photovoltaic power station is zero, which will not affect the system because of the continuous fluctuations in natural energy, like wind turbines.

In terms of the microgrid dispatching strategy, there is no power input from the photovoltaic power station at night as a buffer. Once the wind turbine fluctuates, the power balance of the whole microgrid will be greatly affected. Because, at this time, it can only rely on another limited power supply to adjust, such as energy storage system and micro combustion units, the energy storage system may have problems such as capacity limits, so the impact of the fluctuation of wind turbines on the dispatching operation of the microgrid will be more prominent.

5.3. Calculation and Analysis of Scheduling Potential

Calculate the (35) correlation degree of the data in Table 3 using Equations (28) and (40), calculate the entropy weight using Equation (36), and finally calculate the weighted correlation degree. Among them, ρ = 0.5 represents the traditional grey correlation theory, and the selection of dynamic ρ is an improved grey correlation theory.

(1) Comparative analysis of grey relational theory.

According to Table 4, the improved grey correlation theory effectively weakens the influence of the maximum value of the difference matrix in the calculation of the correlation coefficient by redefining the selection of the resolution coefficient ρ. Meanwhile, as shown in Table 4, the application of the improved algorithm effectively highlights the correlation between the initial investment cost and environmental governance cost with the total operating cost of the microgrid, thereby reflecting the high correlation between the volatility of new energy output and the initial investment cost and environmental governance cost.

Table 4. Comparison of the grey correlation degree for the different algorithms.

Calculation Method	Unit Name	Initial Investment Cost	Equipment Maintenance Cost	Environmental Governance Costs	Weighted Correlation Degree
P = 0.5	Photovoltaic power station	0.882	0.514	0.797	0.716
	Wind turbine unit	0.916	0.559	0.891	0.763
Bender's decomposition algorithm	Photovoltaic power station	0.893	0.496	0.813	0.721
	Wind turbine unit	0.924	0.542	0.899	0.774
Wavelet analysis	Photovoltaic power station	0.887	0.507	0.808	0.718
	Wind turbine unit	0.921	0.549	0.910	0.767
Variable correlation test	Photovoltaic power station	0.914	0.442	0.837	0.732
	Photovoltaic power station	0.937	0.535	0.916	0.791
Dynamic ρ	Photovoltaic power station	0.932	0.413	0.865	0.738
	Wind turbine unit	0.951	0.527	0.929	0.798

(2) Analysis of the correlation between fluctuations in new energy output and various cost indicators.

According to Table 4, the ranking of the degree of correlation between new energy and the initial investment cost, equipment maintenance cost, and environmental governance cost of the local microgrid is as follows: distributed photovoltaic power station > wind turbine. By comparing and analyzing the differences in various cost indicators, the correlation between wind turbines and equipment maintenance costs and environmental governance costs is significantly higher than that of distributed photovoltaic power plants. Therefore, in areas with heavy environmental pollution, the impact of wind turbines in new energy should be fully considered. The correlation between initial investment cost and new energy of wind turbines is slightly greater than that of distributed photovoltaic power plants, so wind turbines should be given special consideration on the basis of similar local photovoltaic and wind energy resources.

(3) Weighted correlation analysis.

According to Table 4, after comprehensive weighting of the cost indicators of new energy and various power grid operations, they are sorted by size as follows: wind turbines > distributed photovoltaic power plants. Therefore, it can be seen that when there is an equal fluctuation in the output of new energy in the region, the cost of wind turbines is greater than that of distributed photovoltaic power plants. Therefore, in the process of long-term planning for new energy in this area, emphasis should be placed on considering the impact of wind turbines on overall operating costs.

(4) Comparative analysis of weighted correlation degree with other algorithms.

According to Table 4, compared to other correlation analysis algorithms, the improved grey correlation theory proposed in this paper can better consider the correlation between initial investment costs and environmental governance costs, resulting in a better initial investment cost, equipment maintenance cost, and environmental governance cost. The weighted correlation degrees of the improved grey correlation theory in this article are 0.738 and 0.798 in the photovoltaic power station and wind turbine unit, respectively.

6. Conclusions

This paper establishes a robust optimization model for the coordinated optimization of new energy sources, energy storage devices, and micro-gas turbine units, with the goal of minimizing the operating cost of the microgrid by using the two-stage robust optimization method. The linearization of the constraint conditions is achieved through the large M method, and the correlation between the new energy and the operating costs as well as the total operating costs of the microgrid are obtained through the improved grey correlation theory and entropy weight method, respectively, to quantitatively analyze the impact of new energy on grid dispatch and identify the key new energy sources affecting microgrid planning. The experimental results show that the improved grey correlation theory optimization scheduling algorithm for new energy microgrids proposed obtains weighted correlation degrees of 0.730 and 0.798 for photovoltaic power stations and wind turbines, respectively, which are 3.1% and 4.6% higher than traditional grey correlation theory. In addition, the equipment maintenance costs of this method are 0.413 and 0.527, respectively, which are 25.1% and 5.4% lower compared with the traditional method, respectively, indicating that the method effectively improves the accuracy of quantitative analysis.

This paper only considers the economic optimality of the integrated system of new energy sources. However, carbon trading is a significant part of the cost, so it should be fully considered and as many new energy sources as possible should be used to fully consider environmental protection issues. Under the guidance of the “dual carbon” goal, the research and practice of optimizing the dispatch of new energy sources are particularly

critical. In the future, it is necessary to deepen the understanding of the characteristics of new energy sources based on existing research and improve the optimization scheduling model to enhance the accuracy and efficiency of the algorithm. At the same time, full consideration should be given to the energy coupling relationship to ensure that the entire system not only achieves the optimal economic efficiency, but also the most environmental protection.

Author Contributions: Conceptualization, F.D.; Data curation, Y.S. and Y.Z.; Formal analysis, D.M.; Investigation, Y.S.; Methodology, Q.L. and F.D.; Resources, Q.L. and Y.Z.; Software, D.M.; Supervision, F.D.; Validation, Q.L., Y.S. and Y.Z.; Writing—original draft, D.M. All authors have read and agreed to the published version of the manuscript.

Funding: This work was supported in part by the Technology Project of Power Dispatch and Control Center, Guangxi Power Grid Grant 046000KK52222033, in part by the National Natural Science Foundation of China under Grant 52362052, 52377103, and in part by the Natural Science Foundation of Jiangxi Province under Grant 20232BAB204065.

Data Availability Statement: The data presented in this study are available in reference [5]. [Bilayer Distributed Optimization for Robust Microgrid Dispatch With Coupled Individual-Collective Profits] [https://doi.org/10.1109/tste.2021.3053559] [5].

Conflicts of Interest: The authors declare no conflict of interest.

Glossary

Variable explanation table.

Variable	Definition
Γ_{wt}	Robustness index characterizes the volatility of uncertain variables of wind turbines
Γ_{pv}	Robustness index characterizes the volatility of uncertain variables in distributed photovoltaic power stations
Γ_{load}	Robustness indicators characterize the volatility of load-uncertain variables
$\boldsymbol{U}$	Uncertain set of boxes with bounded closure
$P^{0}_{\mathrm{wt},t}$	The predicted output power of the wind turbine in period t
$P^{0}_{\mathrm{pv},t}$	Predicted output value of the distributed photovoltaic power station in the t period
$P^{0}_{\mathrm{load},t}$	The predicted demand value for the load during the t period
$P_{\mathrm{wt},t}$	The actual output value of the wind turbine in the period t
$P_{\mathrm{pv},t}$	The actual output value of the distributed photovoltaic power station in the t period
$P_{\mathrm{load},t}$	Demand value of the load during the t period
$\Delta P^{\max}_{\mathrm{wt},t}$	Maximum fluctuation of wind turbines in period t
$\Delta P^{\max}_{\mathrm{pv},t}$	Maximum fluctuation amount of the distributed photovoltaic power station in the t period
$\Delta P^{\max}_{\mathrm{load},t}$	The maximum fluctuation of the load in period t
$r_{\mathrm{wt},t}$	Auxiliary variable with fluctuation upper and lower limit of an uncertain variable
$r_{\mathrm{pv},t}$	Auxiliary variable with fluctuation upper and lower limit of an uncertain variable
$r_{\mathrm{load},t}$	Auxiliary variable with fluctuation upper and lower limit of an uncertain variable
SOC_t	State of charge of the battery during period t
SOC_{t-1}	Charge state of the battery during the t − 1 period
$P^{\mathrm{ch}}_{\mathrm{bat},t}$	Charging power of the battery during period t
$P^{\mathrm{dis}}_{\mathrm{bat},t}$	Discharge power of the battery during period t
η_{ch}	Charging efficiency of the energy storage device
η_{dis}	Discharge efficiency of the energy storage device
E_{EN}	Rated battery capacity
$\chi_{\mathrm{bat},t}$	A 0–1 integer variable
N_{life}	Number of cycles when the battery reaches the upper life limit
$D^{\mathrm{cyc}}_{\mathrm{dod}}$	Discharge depth of the storage battery
N_0	Number of cycles to reach the upper lifetime limit when the battery works at 100% discharge depth
k_p	Fitting coefficient of the power function

k_p	Factory parameters of each battery
N_0	Factory parameters of each battery
$D_{\mathrm{dod},t-1}$	Discharge depth during the t − 1 period
$D_{dod,t-1}^{\mathrm{cyc}}$	Cycle discharge depth in period t
$\chi_{\mathrm{SOC},t}$	A 0–1 integer variable
$\chi_{\mathrm{bat},t}$	A 0–1 integer variable as the number of batteries
$n_{\mathrm{eq},t}$	Equivalent full cycles of the battery during period t
N_{eq}	Daily equivalent full cycles of the battery
C^{inv}	Total initial investment cost of the microgrid
C_{open}	Operation and maintenance costs of the microgrid equipment
$E_{\mathrm{bat}}^{\mathrm{max}}$	Maximum battery capacity of the energy storage device
P_i^{max}	Investment cost of the maximum technical output of the i-th power equipment
c_i	Investment cost per unit power of the i-th power equipment
$F_{\mathrm{CRE}}(r_i, Y_i)$	Annual fund recovery rate
r_i	The discount rate of the i-th electric power equipment
Y_i	The discounted years of the i-th electric power equipment
$C_{\mathrm{G}}^{\mathrm{open}}$	Operating costs of a micro-gas turbine
C_{grid}	Microgrid electricity purchase and sale costs
C_{op}	Maintenance costs of the equipment
$c_{\mathrm{fuel},t}$	Fuel costs during the t time period
$P_{G,t}$	Real-time output of the micro-gas turbine in the t period
$k_{n,t}$	The n th pollutant discharge of the micro-gas turbine in period t
$c_{n,t}$	Unit price of n pollutant treatment of micro-gas turbine in t
$c_{\mathrm{buy},t}$	Unit price of electricity purchased during period t
$c_{\mathrm{sell},t}$	Unit price of electricity sold in the t period
$P_{\mathrm{M},t}^{\mathrm{buy}}$	The power purchased by the microgrid buys from the distribution network during period t
$P_{\mathrm{M},t}^{\mathrm{sell}}$	The power that the microgrid sells to the distribution network during period t
C_{op}^{i}	Maintenance cost unit price of the energy storage device, wind turbine, distributed photovoltaic power station, and micro combustion unit
$P_{i,t}$	Output of energy storage device, wind turbine, distributed photovoltaic power station, and micro combustion unit in the t period
$P_{\mathrm{G}}^{\mathrm{min}}$	Minimum technical output of a micro-gas turbine
$\varepsilon_{\mathrm{ch}}$	Maximum charge and discharge power of energy storage
$\varepsilon_{\mathrm{dis}}$	Ratio of the maximum battery capacity
SOC^{min}	Lower limit of the battery charge state
SOC^{max}	Upper limit of the battery charge state
SOC_{beg}	Initial charge state of the scheduling cycle T battery
SOC_{end}	Final charge state of the T battery during the scheduling cycle
$P_{\mathrm{M}}^{\mathrm{buy,max}}$	The upper limit of the power that the microgrid buys from the distribution network
$P_{\mathrm{M}}^{\mathrm{sell,max}}$	The upper limit of the power that the microgrid sells to the distribution network
$\chi_{\mathrm{M},t}$	A 0–1 integer variable
$Y = (Y_1, Y_2, \ldots, Y_a)$	The a new energy robustness index constitutes the index sequence
$X = (X_1, X_2, \ldots, X_b)$	The index sequence of the dispatching and operation cost composition of the b microgrid
n	Represents the number of economic cost data groups generated after changing the robust coefficient
Δ	Differential matrix
Δ_{ab}	The difference between the robustness index in group a and the economic characteristic index in group b
Δ_{max}	The maximum value of the difference matrix
Δ_{min}	Minimum value of the difference matrix
$\lambda_{ab}(n)$	The association coefficient of the robustness index of group a and the economic characteristic index of group b in row n
ρ	Resolution coefficient, a number between 0–1
r_{ab}	A group of grey correlation of robustness indicators and the economic characteristic index of group b
x_{max}	The maximum value of the X_b
x_{min}	The minimum value of the X_b

T_b	Entroropy of the index in term b
H_b	Entropy weight of the indicators in term b
$D_{\mathrm{dod},n,t}$	The discharge depth of the battery in period t
$D_{\mathrm{dod},n}^{\min}$	Minimum value of the battery discharge depth in period t
$D_{\mathrm{dod},n}^{\max}$	Maximum discharge depth of the battery in period t
$g_{m,t}$	A 0–1 integer variable
x, y, z	Optimize the variable
u	Unsure variable
A, B, E, F, G, H, I, d, h, k	The constant–coefficient matrix of the corresponding constraints
α	Secondary variables of the sub-problem
k	Total number of iterations of the model
y_l, z_l	Solution of the sub-problem after one iteration
u_l	The worst scenario found in an uncertain set after l iterations

References

1. Yang, Y.; Yang, P.; Zhao, Z.; Tang, Y.; Lai, L.L. An Adaptive Optimal Scheduling Strategy for Islanded Micro-Energy Grid Considering the Multiple System Operating States. *IEEE Trans. Sustain. Energy* **2023**, *14*, 393–408. [CrossRef]
2. Qiu, Y.; Li, Q.; Ai, Y.; Chen, W.; Benbouzid, M.; Liu, S.; Gao, F. Two-stage distributionally robust optimization-based coordinated scheduling of integrated energy system with electricity-hydrogen hybrid energy storage. *Prot. Control. Mod. Power Syst.* **2023**, *8*, 1–14. [CrossRef]
3. Qiu, H.; Gu, W.; Xu, X.; Pan, G.; Liu, P.; Wu, Z.; Wang, L. A Historical-Correlation-Driven Robust Optimization Approach for Microgrid Dispatch. *IEEE Trans. Smart Grid* **2021**, *12*, 1135–1148. [CrossRef]
4. Fan, Y.; Wu, X.; Cao, B.; Wang, X. Multi-stage robust feasible region based integrated energy microgrid dispatch. *CSEE J. Power Energy Syst.* **2024**. [CrossRef]
5. Qiu, H.; Gu, W.; You, F. Bilayer Distributed Optimization for Robust Microgrid Dispatch with Coupled Individual-Collective Profits. *IEEE Trans. Sustain. Energy* **2021**, *12*, 1525–1538. [CrossRef]
6. Ye, L.; Mo, Y.; Chen, M.; Chen, X.; Bai, X. Evaluation model on schedulable potential of electric vehicles based on Monte Carlo Simulation. In Proceedings of the 2018 International Conference on Power System Technology (POWERCON), Guangzhou, China, 6–9 November 2018; IEEE: Piscataway Township, NJ, USA; pp. 1–8.
7. Xu, Q.S.; Ding, Y.F.; Yan, Q.G.; Zheng, A.X. Research on evaluation of scheduling potentials and values on large consumers. *Proc. CSEE* **2017**, *37*. [CrossRef]
8. Soroudi, A.; Rabiee, A.; Keane, A. Stochastic Real-Time Scheduling of Wind-Thermal Generation Units in an Electric Utility. *IEEE Syst. J.* **2015**, *11*, 1622–1631. [CrossRef]
9. Ji, G.; Wu, W.; Zhang, B. Robust generation maintenance scheduling considering wind power and forced outages. *IET Renew. Power Gener.* **2016**, *10*, 634–641. [CrossRef]
10. Wang, Z.; Bian, Q.; Xin, H.; Gan, D. A distributionally robust co-ordinated reserve scheduling model considering CVaR-based wind power reserve requirements. *IEEE Trans. Sustain. Energy* **2015**, *7*, 625–636. [CrossRef]
11. Luo, S.; Teng, J.; Tan, Z. Optimization configuration of energy storage in distribution network considering aggregation regulation of electric vehicles. *Energy Storage Sci. Technol.* **2023**, *12*, 3395–3405.
12. Zhang, S.; Wang, B. Shic Collaborative optimization of electric thermal integrated energy distribution network system and hydrogen energy station based on distributed robust optimization. *Electr. Meas. Instrum.* **2023**, *60*, 36–43.
13. Sintaro, S. Penerapan Metode Grey Relational Analysis (GRA) Dalam Pemilihan E-Commerce. *J. Inf. Technol. Softw. Eng. Comput. Sci.* **2023**, *1*, 166–173.
14. Guariglia, E.; Guido, R.C.; Dalalana, G.J.P. From Wavelet Analysis to Fractional Calculus: A Review. *Mathematics* **2023**, *11*, 1606. [CrossRef]
15. Mosele, F.; Deluche, E.; Lusque, A.; Le Bescond, L.; Filleron, T.; Pradat, Y.; Ducoulombier, A.; Pistilli, B.; Bachelot, T.; Viret, F.; et al. Trastuzumab deruxtecan in metastatic breast cancer with variable HER2 expression: The phase 2 DAISY trial. *Nat. Med.* **2023**, *29*, 2110–2120. [CrossRef]
16. Bahabbaz, M.A.; Karim, K. Qualitative Characteristics of Accounting Information (Declared with IFRS Standards) and Financial Performance: Statistical Study and Correlation Test. *Am. J. Econ. Bus. Innov.* **2023**, *2*, 93–100. [CrossRef]
17. Akour, I.; Rahamneh, A.A.L.; Al Kurdi, B.; Alhamad, A.; Al-Makhariz, I.; Alshurideh, M.; Al-Hawary, S. Using the canonical correlation analysis method to study students' levels in face-to-face and online education in Jordan. *Inf. Sci. Lett.* **2023**, *12*, 901–910.

18. Pant, S.; Kumar, A.; Ram, M.; Klochkov, Y.; Sharma, H.K. Consistency indices in analytic hierarchy process: A review. *Mathematics* **2022**, *10*, 1206. [CrossRef]
19. Wu, R.M.; Zhang, Z.; Yan, W.; Fan, J.; Gou, J.; Liu, B.; Wang, Y. A comparative analysis of the principal component analysis and entropy weight methods to establish the indexing measurement. *PLoS ONE* **2022**, *17*, e0262261. [CrossRef] [PubMed]
20. Chowdhury, N.; Katsikas, S.; Gkioulos, V. Modeling effective cybersecurity training frameworks: A delphi method-based study. *Comput. Secur.* **2022**, *113*, 102551. [CrossRef]
21. Zhong, C.; Yang, Q.; Liang, J.; Ma, H. Fuzzy comprehensive evaluation with AHP and entropy methods and health risk assessment of groundwater in Yinchuan Basin, northwest China. *Environ. Res.* **2022**, *204*, 111956. [CrossRef]
22. Bilgili, F.; Zarali, F.; Ilgün, M.F.; Dumrul, C.; Dumrul, Y. The evaluation of renewable energy alternatives for sustainable development in Turkey using intuitionistic fuzzy-TOPSIS method. *Renew. Energy* **2022**, *189*, 1443–1458. [CrossRef]
23. Wang, R.; Wang, P.; Xiao, G. A robust optimization approach for energy generation scheduling in microgrids. *Energy Convers. Manag.* **2015**, *106*, 597–607. [CrossRef]
24. Hosseini, S.M.; Carli, R.; Dotoli, M. Robust optimal energy management of a residential microgrid under uncertainties on demand and renewable power generation. *IEEE Trans. Autom. Sci. Eng.* **2020**, *18*, 618–637. [CrossRef]
25. Wang, X.; Yang, Z.; Liu, F. Construction of a Linear Programming Model for Renewable Energy Microgrid Load Considering Uncertainty. *Microcomput. Appl.* **2023**, *39*, 53–56+60.
26. Wu, J. Research on a Differentiated Planning Model of Power Systems Considering Wind Power Uncertainty. Doctoral Dissertation, Xiangtan University, Xiangtan, China, 2018.
27. Zhang, L.; Li, Y.; Liu, L. State of Health Estimation of Battery Model Based on Parameter Analysis. *Autom. Instrum.* **2022**, *43*, 69–75. [CrossRef]
28. Jian, Z. Estimation Method for Remaining Battery Capacity Based on RBF Neural Network Algorithm. *Equip. Manuf. Technol.* **2019**, *5*, 155–159.
29. Yu, X. Multi-Objective Optimal Scheduling of Microgrids Based on Improved Ant Colony Algorithm. *Hongshui River* **2024**, *43*, 115–121.
30. Tian, D. Research on Optimal Allocation of Shared Energy Storage in Multiple Microgrids Considering Economic Utilization of Renewable Energy. Doctoral Dissertation, Xi'an University of Technology, Xi'an, China, 2024. [CrossRef]
31. Hen, Y. Research on Power Balance Scheduling System and Methods for New Power Systems. Doctoral Dissertation, Harbin Institute of Technology, Harbin, China, 2022. [CrossRef]
32. Ma, L.; Liang, Y.; Cheng, X. Optimal Operation of Microgrid Clusters Considering Networked Energy Storage Stability Expansion. *Electr. Power Eng. Technol.* **2024**, *43*, 214–222.
33. Xie, B.; Wang, X. Analysis of the Relationship Between Water Conservancy Infrastructure Investment and National Economy in Jiangxi Province Based on Grey System Theory. *Water Resour. Hydropower Express* **2023**, *44*, 71–75. [CrossRef]
34. Zhao, G.; Hu, X.; Fang, H. Analysis of the Relationship Between Oyster Mushroom Yield, Quality, and Sugar Beet Pulp Usage Based on Grey System Theory. *Trop. Agric. Sci.* **2022**, *42*, 37–41.
35. Zhou, X.; Ji, C.; Tu, X. Estimation and application of change-point quantile regression model based on linearization technique. *J. Shandong Univ. (Sci. Ed.)* **2024**, 1–8.
36. Yao, W.; Li, W.; Zhang, B. Two-stage robust optimization configuration of a wind-solar-pumped storage joint operation system with fixed/variable speed based on limited rationality. *Electr. Power Autom. Equip.* **2024**, 1–16.
37. Li, Y.; Liu, J.; Ma, Y. Two-Stage Stochastic Robust Optimization of Combined Cooling, Heating, and Power Systems Under Uncertainty. *J. Eng. Thermophys.* **2024**, *45*, 3653–3663.
38. Yao, J.; He, Q.; Zhang, Y.; Xie, Q.; Wang, H.; Deng, L.; Hu, C. Two-Stage Robust Optimization Scheduling Model for Microgrids Considering Wind Power Output Uncertainty. *Zhejiang Electr. Power* **2024**, *43*, 106–115. [CrossRef]